Available online at www.sciencedirect.com

SCIENCE DIRECT

Biochimica et Biophysica Acta 1712 (2005) 128 – 136

BIOCHIMICA ET BIOPHYSICA ACTA
BBA

http://www.elsevier.com/locate/bba

Two-color fluorescent probes for imaging the dipole potential of cell plasma membranes

Vasyl V. Shynkar[a,b], Andrey S. Klymchenko[a], Guy Duportail[a], Alexander P. Demchenko[c], Yves Mély[a,*]

[a]*Laboratoire de Pharmacologie et Physicochimie des interactions cellulaires et moléculaires, UMR 7034 du CNRS, Faculté de Pharmacie, Université Louis Pasteur, 67401 Illkirch, France*

[b]*Department of Physics, Kyiv National Taras Shevchenko University, 01033 Kyiv, Ukraine*

[c]*TUBITAK Research Institute for Genetic Engineering and Biotechnology, Gebze-Kocaeli 41470, Turkey*

Received 23 November 2004; received in revised form 30 March 2005; accepted 31 March 2005
Available online 13 May 2005

Abstract

The dipole potential (Ψ_d) constitutes a large and functionally important part of the electrostatic potential of cell plasma membranes. However, its direct measurement is not possible. Herein, new 3-hydroxyflavone fluorescent probes were developed that respond strongly to Ψ_d changes by a variation of the intensity ratio of their two well-separated fluorescence bands. Using fluorescence spectroscopy with cell suspensions and confocal microscopy with adherent cells, we showed, for the first time, two-color fluorescence ratiometric measurement and visualization of Ψ_d in cell plasma membranes. Using this new tool, a heterogeneous distribution of this potential within the membrane was evidenced.

Keywords: 3-Hydroxyflavone derivative; Cell plasma membrane; Confocal fluorescence microscopy; Dipole potential; Fluorescence probe; Fluorescence spectroscopy

1. Introduction

In contrast to surface [1–3] and transmembrane [4,5] potentials, the dipole potential, Ψ_d, formed between the highly hydrated lipid heads at the membrane surface and the low polar interior of the bilayer does not depend upon the ions at the membrane surface [6,7]. Ψ_d arises from the aligned dipolar groups of phospholipids, with the participation of hydration water molecules, and therefore, it depends strongly on the lipid composition of the bilayer. Ψ_d modifies the electric field inside the membrane, producing a virtual positive charge in the apolar bilayer center. As a result, lipid membranes exhibit a substantial (up to six orders of magnitude) difference in the penetration rates between positively and negatively charged hydrophobic ions [8,9]. Ψ_d plays also an important role in the membrane permeability for lipophilic ions [10] and drugs [11]. Ψ_d was also shown to modulate the binding of peptides [12] and other biologically active molecules [13] to cell plasma membranes, and to direct the insertion and folding of peptides in the membranes [14]. Finally, changes in Ψ_d may also modulate membrane enzyme activities [15,16].

Since Ψ_d propagates from the middle of the bilayer to the interface, its direct measurement is not possible, and fluorescence probes with electrochromic properties offer an unique opportunity for its nondestructive study [17]. Styrylpyridinium probes respond to Ψ_d changes by a significant shift of their excitation spectrum [6,7,18,19]. This allows ratiometric recording, provided that the sample could be excited with two different wavelengths. Since this possibility could not be easily achieved with most fluorescence microscopes, it would be much more convenient to dispose of dyes with ratiometric response in emission that would be ideally adapted for multi-color imaging micro-

* Corresponding author.
E-mail address: mely@aspirine.u-strasbg.fr (Y. Mély).

0005-2736/$ - see front matter © 2005 Elsevier B.V. All rights reserved.
doi:10.1016/j.bbamem.2005.03.015

scopes. Indeed, using a single wavelength excitation, the emission of these dyes can be collected on two separate detectors using appropriate broad-band filters. Moreover, fluorescence ratiometric measurements eliminate distortions of data caused by photobleaching and variations in probe loading and retention, as well as by instrumental factors such as illumination stability and sensitivity of the detector [20,21]. Some successful attempts have been made to provide two-color fluorescence microscopy recordings with styrylpyridinium probes [22]. However, their relatively weak response to Ψ_d in fluorescence emission as compared to that in excitation [6,19] limits their applications for this microscopy technique. In this context, our aim was to design Ψ_d-sensitive probes by using 3-hydroxyflavone dyes which exhibit two emission bands well separated on the wavelength scale. In a number of model systems, it was shown that the electrochromic and solvatochromic shifts of these two bands are connected with strong changes of their relative intensities [23–25]. In our previous study [26], two probes, BPPZ and F4N1 (Fig. 1), were synthesized to measure Ψ_d in model phospholipid vesicles. BPPZ is oriented by its chromone ring towards the center of the bilayer, while F4N1 is oriented in the opposite direction. The excitation and emission bands shift in accordance with the probe orientation in the bilayers and with variations of Ψ_d induced by the substitution of ester lipids by their ether analog or by the incorporation of Ψ_d modifiers like phloretin and 6-ketocholestanol. Importantly, these shifts are accompanied by strong changes in the intensity ratio of the two emission bands, suggesting that Ψ_d may be visualized in living cells by wavelength-ratiometric imaging. We designed and synthesized herein two novel probes, PPZ8 and F8N1S (Fig. 1), which exhibit the same basic properties than the previous ones [26] but show higher affinity and selectivity towards the cellular plasma membrane. Spectrofluorometric experiments with cell suspensions and confocal fluorescence imaging of individual cells demonstrate strong ratiometric response of the novel probes to variation of dipole potential.

2. Materials and methods

2.1. Cells

THP-1 cells, a human acute monocytic leukemia line, were obtained from the American Type Culture Collection and grown in RPMI medium supplemented with β-mercaptoethanol (20 μM), 1% antibiotic streptomycin/penicillin, and 10% fetal bovine serum. For staining, the cells were centrifuged and resuspended in Hank's balanced salt solution (HBSS), 0.05% Pluronic F127, and 1 μM PPZ8, F8N1S, or di-8-ANEPPS. The cell suspension was placed in a shaker bath for 10 min in the incubator, washed once in probe-free HBSS containing 0.05% Pluronic F127, and finally in HBSS alone. Stained cells were resuspended at a concentration of 10^6 cells/ml for fluorescence analysis. The staining pattern of the cells was checked with a Confocal Imaging System MRC-1024 (BioRad) to ascertain that the fluorescence originates from the plasma membrane.

L929 cells, a mouse fibroblast line, were obtained from the American Type Culture Collection and grown in

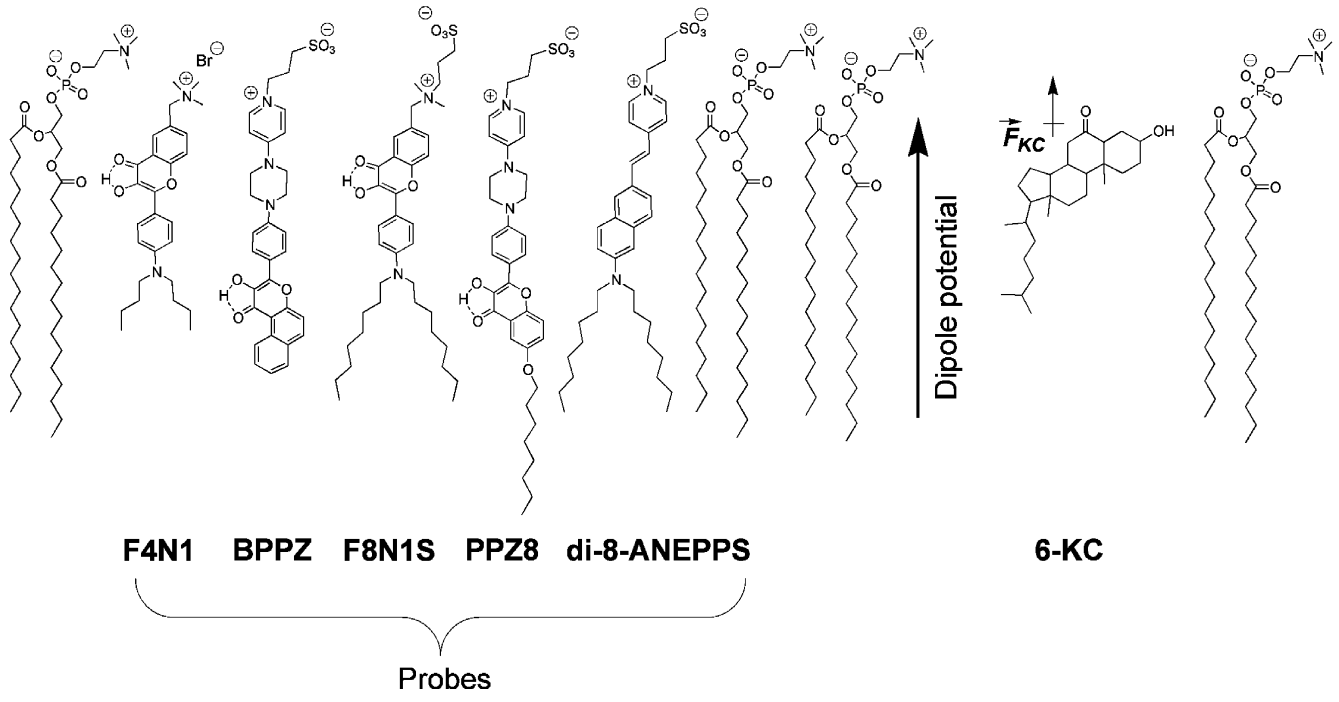

Fig. 1. Fluorescent probes used in the present study and their expected location in phospholipid bilayers. The large arrow shows the direction of Ψ_d (positive inside the bilayer), and the small arrow shows the contribution of 6-KC to Ψ_d.

Dulbecco's MEM Seromed media supplemented with 1% sodium pyruvate, 0.5% antibiotic streptomycin/penicillin, and 10% fetal bovine serum. For confocal laser microscopy measurements, the cells were prepared in Lab-Tek II 2-well chambered coverglass, with 10^5 cells/well. For staining, the cells were washed with 2 ml of HBSS, 0.05% Pluronic F127, and 1 μM of PPZ8 (or F8N1S). The chambered coverglass was placed in a shaker bath for 10 min, washed once in probe-free HBSS containing 0.05% Pluronic F127, and finally in HBSS alone.

2.2. Chemicals

Cholesterol, 6-ketocholestanol (6-KC), and pluronic F-127 were purchased from Sigma and used without further purification. RPMI and fetal bovine serum were from Sigma. Dulbecco's MEM 1× was from Biochrom AG, HBSS was from Gibco BRL, and antibiotic streptomycin/penicillin and sodium pyruvate were from Cambrex. Probe 1-(3-sulfonatopropyl)-4-[β [2-(di-*n*-octylamino)-6-napthyl]-vinyl]pyridium betaine (di-8-ANEPPS) was from Molecular Probes (Eugene, USA).

2.3. Synthesis of new probes

The probe PPZ8 (3-(4-{4-[4′-(3-hydroxy-6-octyloxy-flavonyl)phenyl] piperazino}-1-pyridiniumyl)-1-propane-sulfonate) was prepared in three steps, starting from 2′-hydroxy-4′-octyloxyacetophenone (prepared from 2′,4′-dihydroxyacetophenone and octyl iodide) and 4-[4-(4-pyridyl)piperazino]benzaldehyde as described previously for its parent analog PPZ (4-{4-[4′-(3-hydroxyflavonyl)]-piperazino}-1-(3-sulfopropyl)pyridinium) [30] and purified by recrystallization from DMF. ^{1}H NMR and mass data correspond to the structure.

The probe F8N1S 3-[2-(4-(dioctylamino)-3-hydroxyflavonylmethyl)(dimethyl)ammonio]-1-propanesulfonate was prepared in five steps starting from 4′-chloromethyl-2′-hydroxyacetophenone and 4-(dioctylamino)benzaldehyde (prepared in two steps from octyl iodide and aniline). First, a reactive intermediate 6-bromomethyl-4′-(dioctylamino)-3-hydroxyflavone was prepared in three steps using a procedure described previously for its 4′-(diethylamino)-analog [30]. On the next step, this intermediate was converted into 6-dimethylaminomethyl-4′-(dioctylamino)-3-hydroxyflavone using dimethyl amine in THF. The reaction of the latter with 1,3-propane sulton in DMF afforded F8N1S. The probe was purified using thin layer chromatography on silica gel eluted with dichloromethane/methanol, 5/1, v/v. ^{1}H NMR and mass data correspond to the structure.

2.4. Modification of dipole potential in cell membranes

To modify Ψ_d in THP-1 and L929 cells, a DMSO stock solution containing 7.5% Pluronic F127 with 2.5 mM 6-KC was prepared. Aliquots from this stock solution was added to a continuously stirred THP-1-labeled cell suspension directly into the spectrofluorimeter cuvette, allowing 3-min incubation at room temperature for full equilibration before spectra recording. In the case of L929 cells, HBBS with a 2.5 mM concentration of 6-KC was added to washed cells in Lab-Tek II 2-well chambered coverglass and incubated for 3 min.

2.5. Spectroscopic measurements

Absorption spectra were measured on a Cary 400 (Varian) spectrophotometer. Fluorescence spectra were recorded on a FluoroMax-3 (JobinYvon Horiba) spectrofluorometer. The emission wavelengths for fluorescence excitation spectra were 620 nm for probe di-8-ANEPPS and 570 nm for PPZ8 and F8N1S. The excitation wavelength for the fluorescence emission spectra of probe PPZ8 and F8N1S was 400 nm. All spectra were corrected for lamp intensity variations, dilution, and signals from the blank.

2.6. Fluorescence imaging

For collecting cell images, a Laser Scanning Confocal Imaging System MRC-1024 (Bio-Rad) was used. Cells in chambered coverglass were prepared as described above. The 442-nm line of a HeCd laser was used as the excitation light source. Emission was collected by using two filters: 485/30 for the N* band and 585LP for the T* band. The intensity values of the collected images were smoothed by 5×5 pixels, using the confocal assistant software (CAS 40). Digital filters (Amira 3.0 software) were then used to exclude noisy blank pixels from further calculations. These pixels correspond to points in the extracellular medium or within the cytoplasm or nucleus where the dye concentration is very low. Finally, a pixel-by-pixel division of the two images was performed to obtain the intensity ratios between the N* and T* bands and thus spatially resolve the dipole potential changes in the membrane.

3. Results and discussion

3.1. Development of new probes with high selectivity to cell plasma membranes

As a first step, we performed confocal laser microscopy on adherent L929 cells stained with probes of first generation, F4N1 and BPPZ [26]. The obtained fluorescence images reveal crucial drawbacks of these probes: rapid penetration of F4N1 inside the cells and low brightness of BPPZ (data not shown). To overcome these problems, we designed two new molecules, F8N1S and PPZ8 (Fig. 1), which are improved analogs of the F4N1 and BPPZ probes, respectively. Probe F8N1S, with respect to its parent analog F4N1, possesses a zwitterionic group and

longer hydrocarbon chains, which should significantly diminish the penetration rate of the probe through the bilayer. On the other hand, in PPZ8, one benzene ring of BPPZ was substituted with a 6-octyloxy group to improve the structural fit of the probe with the lipid components of the membranes.

Images obtained by confocal laser microscopy of adherent L929 cells stained with probes F8N1S and PPZ8 (Fig. 2a and b) demonstrate emission exclusively from the plasma membranes. An excellent selectivity of the new probes for cell plasma membranes is also observed with THP-1 cells in suspension (Fig. 2a and b, insets). Importantly, the probes stay in the membrane during the whole observation time under the microscope (data not shown), which is limited by the lifetime of the cells in the HBBS buffer (approx. 1 h). Moreover, both the F8N1S and PPZ8 probes were found to be sufficiently bright for visualizing individual cells. We also observe some inhomogeneity in the distribution of the fluorescence intensity at the plasma membrane. This is probably connected with the heterogeneous lipid distribution in the bilayer that affects the probe distribution.

3.2. Response of the new dyes to dipole and surface potential in lipid vesicles

To test the response of the F8N1S and PPZ8 probes to the dipole potential in model systems, we used large unilamellar vesicles (LUV) of different composition. An increase of the dipole potential in the lipid bilayer can be induced by the addition of 6-KC. The addition of 30% of 6-KC into DOPC vesicles labeled by F8N1S induces a 5-nm blue shift in the excitation spectrum of this probe (Fig. 3a). Moreover, in the fluorescence spectrum, we observe a 2-nm blue shift of the N* band, which is accompanied by a 2-fold decrease in the I_{N*}/I_{T*} ratio (Fig. 3a). To obtain a decrease of the dipole potential, DMPC lipids were substituted by

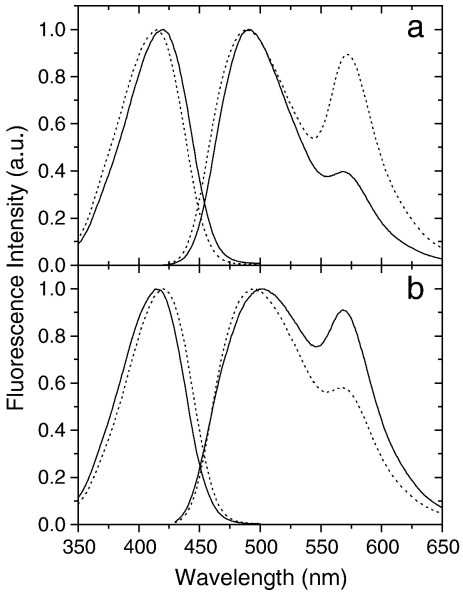

Fig. 3. Excitation and emission fluorescence spectra of the F8N1S dye in phospholipid vesicles: (a) DOPC (solid line) and mixture of DOPC and 30% 6-KC (dot line). (b) DMPC (solid line) and DTPC (dot line).

their ether analogues DTPC. As expected, all the spectroscopic effects in this case were opposite to those observed with 6-KC since both a red shift of the excitation spectrum and an increase in the I_{N*}/I_{T*} ratio were evidenced (Fig. 3b). The response of probe F8N1S to variations of dipole potential is in line with the responses of the analog probe F4N1 and the potentiometric probe di-8-ANEPPS [6,26]. In addition, PPZ8, which exhibits an orientation opposite to F8N1 in the lipid bilayer, demonstrates exactly opposite spectroscopic effects, in line with the corresponding data for its analog BPPZ [25]. In this study, phloretin could not be used as a dipole potential modifier, since it induces some perturbations of the fluorescence spectra of both dyes (data not shown), suggesting a specific interaction between these dyes and phloretin. This interaction is probably due to the

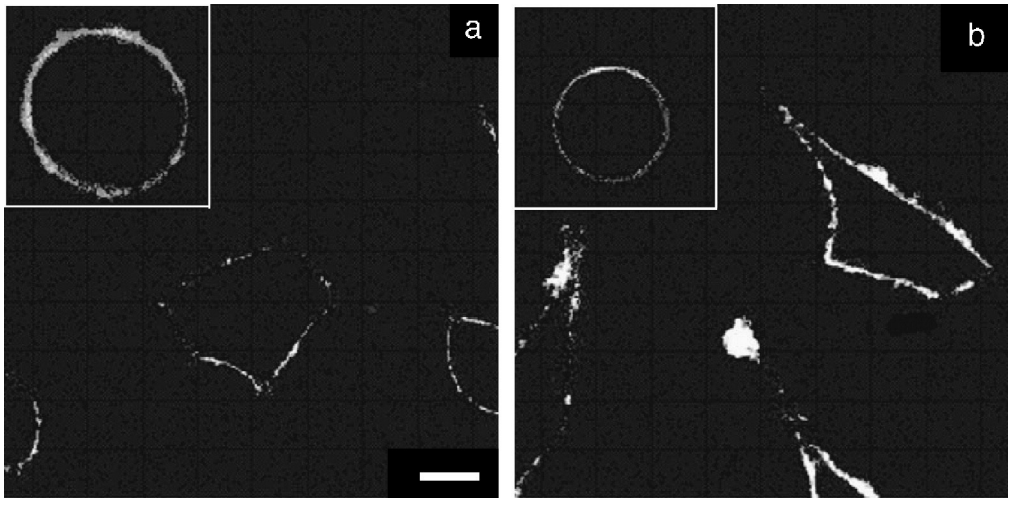

Fig. 2. Fluorescence images of L929 cells stained with probes F8N1S (a) and PPZ8 (b). All images were obtained by collecting fluorescence in the 585–700 nm wavelength range 10 min after probe addition. Inserts were obtained with THP-1 cells. Scale bar, 10 μm (a).

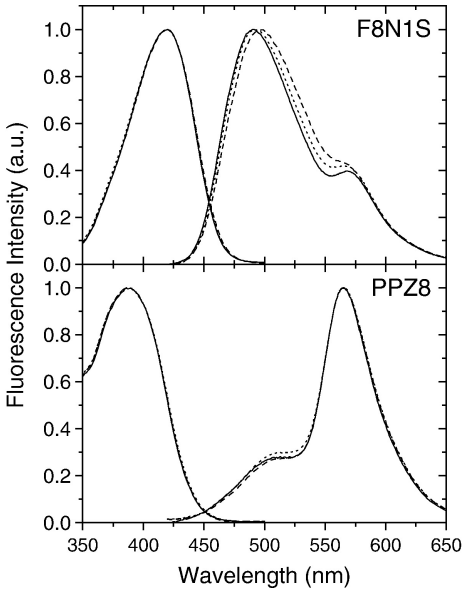

Fig. 4. The excitation and emission spectra of F8N1S and PPZ8 in DOPC (solid line), DOPG (dash line) and DOPS (dot line) vesicles.

formation of an H-bond between the carbonyl group of 3-hydroxyflavones and the hydroxyl groups of phloretin [23].

Importantly, both the F8N1S and PPZ8 probes appear poorly sensitive to an increase of the negative charge on the LUV surface (Fig. 4) since the excitation and emission spectra of these probes are very close in neutral (DOPC) and anionic (DOPG and DOPS) vesicles. The low sensitivity of F8N1S and PPZ8 to surface potential could be explained by their deep location in the lipid bilayers and, therefore, their significant screening from the membrane surface. The pH effect on the fluorescence spectra of the new probes in lipid vesicles was also checked. The spectroscopic characteristics of both probes remain unchanged in the pH range 5 to 9. Thus, being insensitive to pH variations in the physiological range and poorly sensitive to the surface potential, the new probes F8N1S and PPZ8 demonstrate a good selectivity to dipole potential in lipid bilayers.

3.3. Measurements of membrane dipole potential in cell suspensions

The dipole potential of THP-1 cells was modulated by the addition of 6-ketocholestanol (6-KC, see Fig. 1) [9]. As a reference probe, we used di-8-ANEPPS [6] (Fig. 1). We observe that, with the addition of 6-KC to the THP-1 monocytes, the maximum of the excitation spectrum of this probe shifts to the blue (Fig. 5a), in line with the results obtained on model membranes and L1210 cells [6]. This effect reaches a plateau at 20 μM of 6-KC.

Using the same protocol, the excitation spectra of probes PPZ8 and F8N1S were recorded (Fig. 5a). As for di-8-

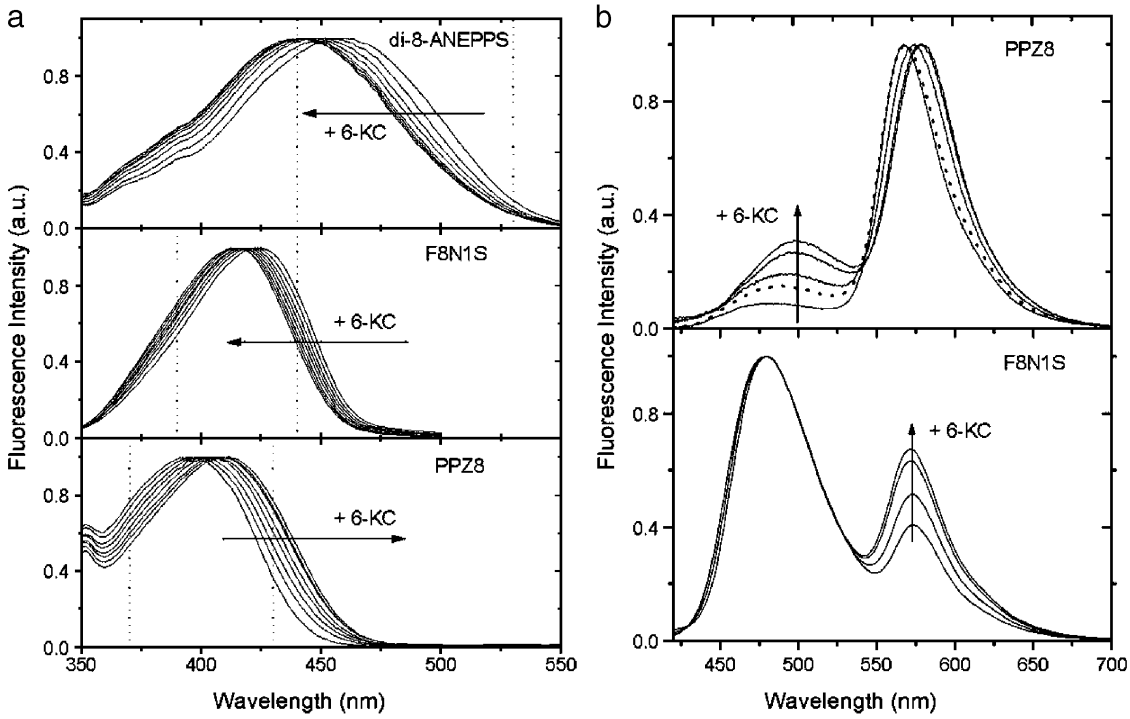

Fig. 5. Response in excitation (a) and emission (b) spectra of di-8-ANEPPS, F8N1S and PPZ8 to variations of the dipole potential in THP-1 cell plasma membrane produced by the addition of 6-KC. (a) The spectra were recorded at the following emission wavelengths: 620 nm for di-8-ANEPPS and 570 nm for PPZ8 and F8N1S. The spectra were normalized at the band maximum. The directions of the spectral shifts are shown by arrows and are the result of adding increasing concentrations of 6-KC (5, 10, 15, 20, 30, 40, and 50 μM). The vertical dotted lines indicate the wavelengths used for ratiometric measurements: 440 nm and 530 nm for di-8-ANEPPS, 390 nm and 440 nm for F8N1S, and 370 nm and 430 nm for PPZ8. (b) Ψ_d was modified by the addition of 6-KC to final concentrations of 10, 20, and 40 μM (the increase is shown by arrows). The spectra were normalized at the T* band for PPZ8 and at the N* band for F8N1S. The dotted line in the upper panel shows the effect of the addition of 50 μM cholesterol.

ANEPPS [6], the addition of 6-KC results in a blue shift of the excitation spectrum of F8N1S. This was expected since the dipole moments of the F8N1S and di-8-ANEPPS fluorophores orient parallel to the dipole potential vector in the bilayer (Fig. 1), giving an energy increase (blue shift) on an increase of Ψ_d. Meanwhile, for PPZ8, we observe a red shift of the excitation spectrum with the addition of 6-KC (Fig. 5a), in line with the opposite orientation of its fluorophore with respect to F8N1S (Fig. 1). Noticeably, the saturation of the spectral effect for the new probes is reached at a higher 6-KC concentration (50 μM) than with di-8-ANEPPS (20 μM), suggesting a stronger interaction of 6-KC with di-8-ANEPPS than with the new probes.

The main advantage of 3HF dyes in comparison with di-8-ANEPPS is the presence of two well-separated fluorescence bands whose ratio is very sensitive to changes in electric fields [23,26]. This allows performing ratiometric measurements with the emission spectra, which is much more precise and convenient than ratiometric measurements on the slopes of the excitation spectra. The emission spectra of both F8N1S and PPZ8 in THP-1 cells are given in Fig. 5b. The short-wavelength band (with a maximum at 479 nm for F8N1S and at 484 nm for PPZ8) corresponds to the excited state normal (N*) form, while the long-wavelength band (with a maximum at 573 nm for F8N1S and at 570 nm for PPZ8) corresponds to the tautomer (T*) form that results from the excited-state intramolecular proton transfer reaction.

The addition of the Ψ_d modifier, 6-KC, changes dramatically the fluorescence spectra of both 3-HF probes (Fig. 5b). For F8N1S, the increase in Ψ_d results in a strong increase of the relative intensity of the T* band and in small blue shifts of both emission bands. As expected, the changes in the emission spectrum of probe PPZ8 are exactly opposite, namely an increase of the N* band relative intensity and red shifts of both the N* (from 484 nm to 502 nm) and T* (from 570 nm to 581 nm) bands are observed (Fig. 5b). These opposite spectroscopic responses of dyes with opposite orientation in the bilayer provide a direct evidence that these probes are sensitive to Ψ_d, which is a vectorial property of the bilayer. In line with previous data on the spectroscopic properties of 3-hydroxyflavone dyes [24,27], the correlation between the shifts of the fluorescence emission bands and the strong variation of their relative intensities is probably related to the coupling of the relative energies of the N* and T* states (reflected by their emission band positions) with their relative populations at equilibrium (reflected by the relative band intensities) [24,25]. This produces a strong amplification effect resulting in a dramatic change of emission color. Noticeably, the saturation effect of 6-KC, observed in the excitation spectra of both probes, is also seen in the fluorescence spectra at the same 6-KC concentration (50 μM).

To further check the specificity of the probe response to Ψ_d changes, cholesterol was added to THP-1 cells labeled with PPZ8. Cholesterol strongly modifies several bilayer properties but affects Ψ_d only to a very small extent [6]. We observe that in contrast to 6-KC, cholesterol produces only a small increase of the relative intensity of the N* band of PPZ8 (Fig. 5b). Thus, probe PPZ8 demonstrates selectivity to dipole potential variation and does not sense the changes in the bilayer properties produced by cholesterol.

Taking into account the difficulty to perform absolute measurements of Ψ_d in voltage units, the use of our probes for measuring Ψ_d changes was validated by investigating the quantitative correlation between the responses of di-8-ANEPPS taken as a reference, and our probes to the addition of 6-KC in TPH-1 cell suspensions. For di-8-ANEPPS, the Ψ_d changes are inferred from the shifts of the excitation spectrum by measuring the intensity ratio, I_{440}/I_{530}, at the two opposite slopes of the spectrum [6]. For our probes, the Ψ_d changes can be evaluated from the excitation spectra shifts in the same way. For this comparison, we chose for F8N1S the ratio of intensities at 390 and 440 nm (I_{390}/I_{440}). Since the response for PPZ8 is in the opposite direction, a reversed ratio was used for this probe, I_{430}/I_{370}. As seen in Fig. 6a, the correlation of these ratios with that of di-8-ANEPPS in the tested range of 6-KC concentrations (0–20 μM) is excellent.

To quantitatively measure the fluorescence response of the new probes to Ψ_d, the intensity ratios at the emission maxima of their two bands can also be used. Thus, we selected I_{570}/I_{480} for F8N1S and a reverse ratio, I_{510}/I_{580}, for PPZ8. Again, an excellent correlation between the ratio-

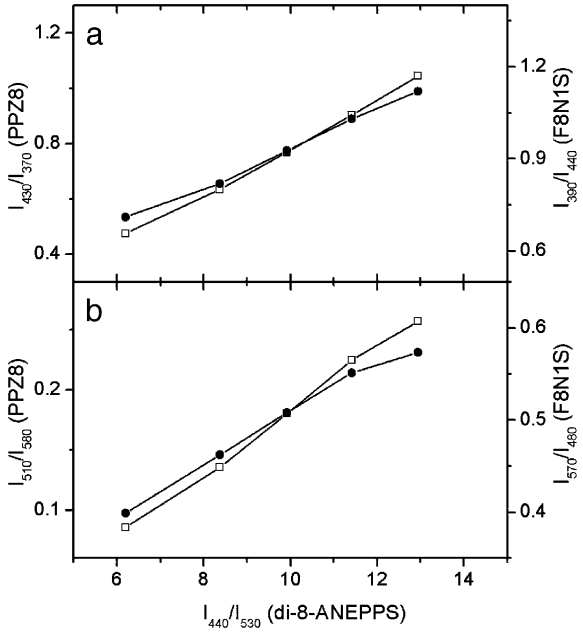

Fig. 6. Correlation of the ratiometric response in the excitation (a) and emission (b) spectra of probes PPZ8 (□) and F8N1S (●) with the ratiometric response in the excitation of di-8-ANEPPS in THP-1 cell suspensions. Correlation curves were built for final 6-KC concentrations of 0, 5, 10, 15, and 20 μM.

metric response in the emission of the new probes and the ratiometric response in the excitation of di-8-ANEPPS was observed (Fig. 6b), validating their applicability for fluorescence ratiometric measurements of Ψ_d. It is important to note that both in the excitation and emission spectra, the ratiometric response of probe PPZ8 is larger than that of F8N1S. This is probably connected with the differences in the location depths of these two probes. Indeed, the chromone moiety of PPZ8 locates deeper in the membrane and is thus closer to the location of the dipole potential modifier 6-KC.

As a consequence, we demonstrate that the response of the newly synthesized 3-HF probes to Ψ_d in excitation spectra is accompanied by strong changes of the relative intensities of their two well-separated spectral bands in emission. This strong response in fluorescence emission is an important advantage of the new probes as compared with di-8-ANEPPS. Furthermore, we found that the fluorescence response of the new probes to the dipole potential correlates linearly with the response of di-8-ANEPPS, so that it correlates linearly with the Ψ_d value itself. These results indicate the possibility to perform color imaging of Ψ_d in cells using fluorescence microscopy.

3.4. Ratiometric imaging of dipole potential in living cells

Two-color confocal fluorescence microscopy of L929 living cells stained with F8N1S and PPZ8 was performed. The emission light was collected in two spectral regions: at 470–500 nm, to monitor the emission of the N* band, and above 585 nm, to collect the emission of the T* band. Ratiometric images were obtained by dividing the intensity of the N* band by the intensity of the T* band and were used to monitor the dipole potential changes induced by the addition of 6-KC (Figs. 7 and 8a and b).

With the addition of 5 μM of 6-KC, the intensity ratio of PPZ8 increases up to three times (Fig. 7a and b), in line with the ratio changes observed with cell suspensions (Fig. 5b). Moreover, as expected, the addition of the same amount of 6-KC decreases the intensity ratio of F8N1S by two times (Fig. 8a and b). The changes of the two-band intensity ratio

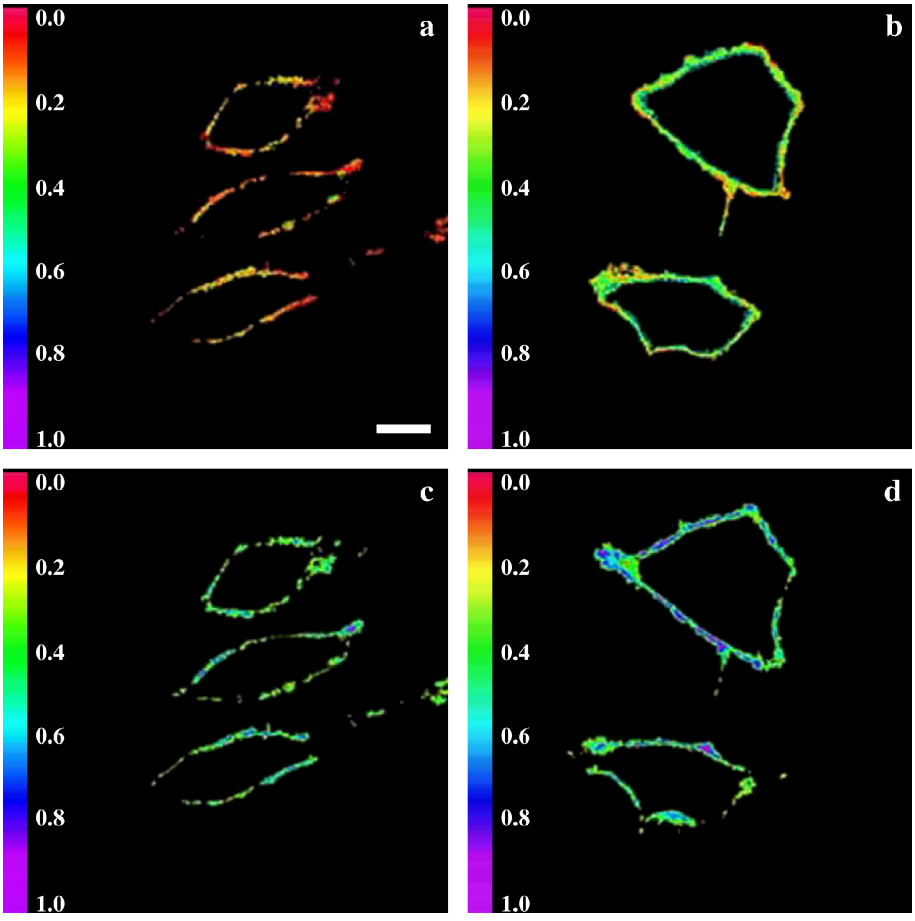

Fig. 7. Confocal fluorescence images of PPZ8 in L929 cells. The images were recorded after a 10-min incubation of the probe with the cells. (a and b) Ratiometric imaging. The ratios of the intensities of the N* band to those of the T* band are displayed in pseudocolor by using the color code on the left scale. (c and d) Intensity imaging. The emission intensity (in relative units) from the T* band of PPZ8 is presented in pseudocolor by using the color code on the left scale. In panels b and d, 6-KC was added to the cells to a final concentration of 5 μM. Scale bar, 10 μm.

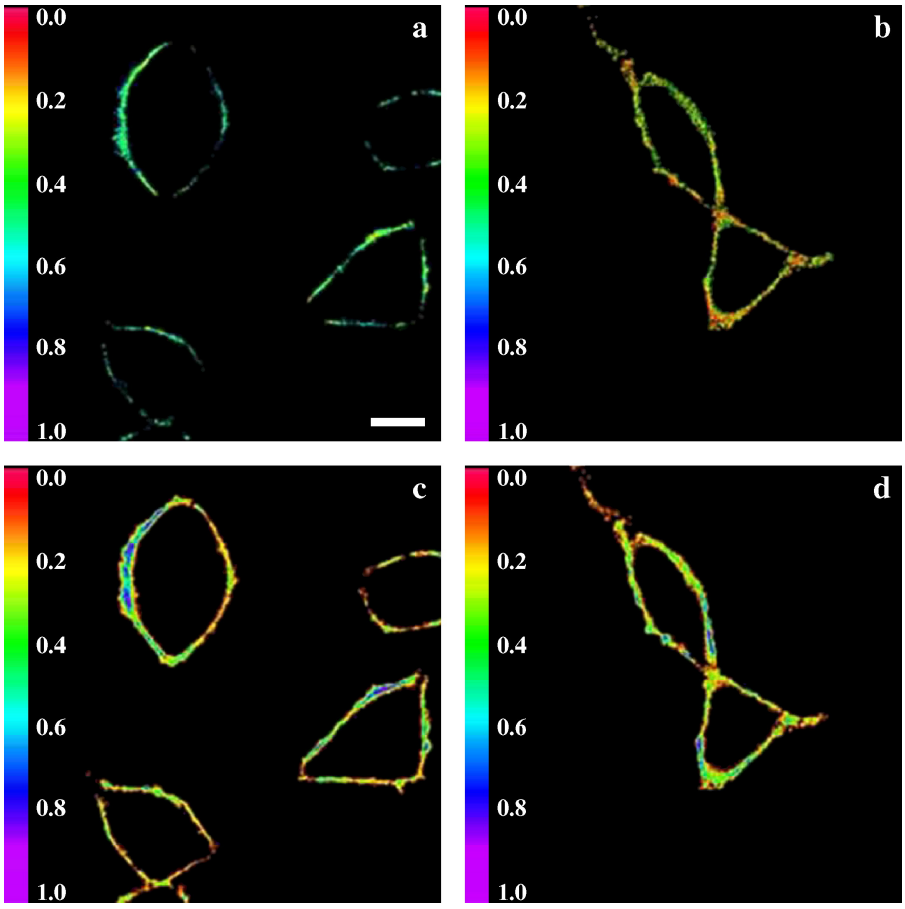

Fig. 8. Confocal fluorescence images of F8N1S in L929 cells. The images were recorded after a 10-min incubation of the probe with the cells. The experimental conditions and expression of the results are as in Fig. 7. Scale bar, 10 μm.

in opposite directions for these two probes are in line with the results obtained on cell suspensions. Thus, probes PPZ8 and F8N1S provide strong and well-detectable ratiometric response to changes of the membrane dipole potential on a single cell level.

Though the average ratio obtained from different cells was more or less constant, heterogeneity on the local values of this ratio can be noticed within the membrane of a given cell both before and after the addition of 6-KC (Figs. 7a and b; 8a and b).

This heterogeneity is not due to autofluorescence since the latter was checked to be negligible (less then 5%) in respect with the fluorescence of the probes. Moreover, we observe also no correlation between local fluorescence intensities (Figs. 7c and d; 8c and d) and local intensity ratios for both probes (Figs. 7a and b; 8a and b), suggesting that variations in the probe concentration within the membrane are not responsible for the heterogeneity in the intensity ratios.

Therefore, this heterogeneity may be due to variation of the lipid composition within the plasma membrane, as well as to the heterogeneous distribution of membrane proteins that may modulate Ψ_d at different parts of the plasma membrane.

4. Conclusions

We developed herein, for the first time, two-color fluorescent probes for ratiometric imaging of membranes in living cells. These dyes were designed on the basis of the 3-hydroxyflavone fluorophore that undergoes an excited state intramolecular proton transfer (ESIPT) and exhibits two highly emissive and well-separated fluorescence bands. The synthesized probes show selective and strong two-band ratiometric response in fluorescence spectra to variation of dipole potential in cell plasma membranes. This is a major advantage over the commonly used voltage-sensitive styrylpyridinium probes that show ratiometric response in excitation spectra. Thus, the new dyes are ideally adapted for multi-color imaging microscopy. Indeed, using a single wavelength excitation, the emission of the dyes can be collected on two separate detectors using appropriate broad-band filters, allowing an efficient collection of emission quanta from the probe. As the ratio of the two emission bands is recorded, the signal will depend neither on instrumental factors (such as fluctuations of light source intensity or sensitivity of the detector) nor upon the absolute probe concentration [20,21]. The high sensitivity of the new probes reveals some heterogeneity of the dipole potential

within the cell plasma membrane, which may be connected with the heterogeneity of its lipid and protein composition. Moreover, since ESIPT is a very fast process (picosecond range), the dyes will enable real-time recording of Ψ_d changes at a sub-cellular level. An additional advantage of these probes is that their two-band emission provides more spectroscopic information than single band probes do [24]. This should enable a simultaneous characterization of several additional properties of lipid membranes, such as polarity and hydration [28,29], providing, thus, an important and powerful tool to characterize different functional states of the living cells.

Acknowledgements

We wish to thank Prof. Maurice Goeldner and Dr. André Mann for providing support for organic synthesis. This work was supported by the TUBITAK Research Institute for Genetic Engineering and Biotechnology (Turkey) and by CNRS (France). APD was a fellow from the French Ministère de la Recherche and Collège Doctoral Européen. ASK is a fellow from the European project TriOH. VVS is a student of Collège Doctoral Européen and is supported by the Région Alsace.

References

[1] G. Cevc, Membrane electrostatics, Biochim. Biophys. Acta 1031 (1990) 311–382.
[2] M. Langner, K. Kubica, The electrostatics of lipid surfaces, Chem. Phys. Lipids 101 (1999) 3–35.
[3] W.W. Wilson, M.M. Wade, S.C. Holman, F.R. Champlin, Status of methods for assessing bacterial cell surface charge properties based on zeta potential measurements, J. Microbiol. Methods 43 (2001) 153–164.
[4] H.M. Shapiro, Cell membrane potential analysis, Methods Cell Biol. 41 (1994) 121–133.
[5] W.Y. Kao, C.E. Davis, Y.I. Kim, J.M. Beach, Fluorescence emission spectral shift measurements of membrane potential in single cells, Biophys. J. 81 (2001) 1163–1170.
[6] E. Gross, R.S. Bedlack Jr., L.M. Loew, Dual-wavelength ratiometric fluorescence measurement of the membrane dipole potential, Biophys. J. 67 (1994) 208–216.
[7] R.J. Clarke, The dipole potential of phospholipid membranes and methods for its detection, Adv. Colloid Interface Sci. 89–90 (2001) 263–281.
[8] E.A. Liberman, V.P. Topaly, Permeability of bimolecular phospholipid membranes for fat-soluble ions, Biofizika 14 (1969) 452–461.
[9] J.C. Franklin, D.S. Cafiso, Internal electrostatic potentials in bilayers: measuring and controlling dipole potentials in lipid vesicles, Biophys. J. 65 (1993) 289–299.
[10] V.L. Sukhorukov, M. Kurdchner, S. Dilsky, T. Lisec, B. Wagner, W.A. Schenk, R. Benz, U. Zimmermann, Phloretin-induced changes of lipophilic ion transport across the plasma membrane of mammalian cells, Biophys. J. 81 (2001) 1006–1013.
[11] J. Cladera, P. O'Shea, J. Hadgraft, C. Valenta, Influence of molecular dipoles on human skin permeability: use of 6-ketocholestanol to enhance the transdermal delivery of bacitracin, J. Pharm. Sci. 92 (2003) 1018–1027.
[12] L. Voglino, T.J. McIntosh, S.A. Simon, Modulation of the binding of signal peptides to lipid bilayers by dipoles near the hydrocarbon–water interface, Biochemistry 37 (1998) 12241–12252.
[13] T. Asawakarn, J. Cladera, P. O'Shea, Effects of the membrane dipole potential on the interaction of saquinavir with phospholipid membranes and plasma membrane receptors of Caco-2 cells, J. Biol. Chem. 276 (2001) 38457–38463.
[14] J. Cladera, P. O'Shea, Intramembrane molecular dipoles affect the membrane insertion and folding of a model amphiphilic peptide, Biophys. J. 74 (1998) 2434–2442.
[15] B. Maggio, Modulation of phospholipase A2 by electrostatic fields and dipole potential of glycosphingolipids in monolayers, J. Lipid Res. 40 (1999) 930–939.
[16] C. Xu, L.M. Loew, Activation of phospholipase C increases intramembrane electric fields in N1E-115 neuroblastoma cells, Biophys. J. 84 (2003) 4144–4156.
[17] L.M. Loew, Spectroscopic Membrane Probes, vol. 1, CRC Press, Boca Raton FL, USA, 1988.
[18] R.J. Clarke, D.J. Kane, Optical detection of membrane dipole potential: avoidance of fluidity and dye-induced effects, Biochim. Biophys. Acta 1323 (1997) 223–239.
[19] R.J. Clarke, Effect of lipid structure on the dipole potential of phosphatidylcholine bilayers, Biochim. Biophys. Acta 1327 (1997) 269–278.
[20] G.R. Bright, G.W. Fisher, J. Rogowska, D.L. Taylor, Fluorescence ratio imaging microscopy, Methods Cell Biol. 30 (1989) 157–192.
[21] R.B. Silver, Ratio imaging: practical considerations for measuring intracellular calcium and pH in living tissue, Methods Cell Biol. 56 (1998) 237–251.
[22] A. Bullen, S.S. Patel, P. Saggau, High-speed, random-access fluorescence microscopy: I. High-resolution optical recording with voltage-sensitive dyes and ion indicators, Biophys. J. 73 (1997) 477–491.
[23] A.S. Klymchenko, A.P. Demchenko, Electrochromic modulation of excited-state intramolecular proton transfer: the new principle in design of fluorescence sensors, J. Am. Chem. Soc. 124 (2002) 12372–12379.
[24] A.S. Klymchenko, A.P. Demchenko, Multiparametric probing of intermolecular interactions with fluorescent dye exhibiting excited state intramolecular proton transfer, Phys. Chem. Chem. Phys. 5 (2002) 461–468.
[25] V.V. Shynkar, Y. Mely, G. Duportail, E. Piemont, A.S. Klymchenko, Picosecond time-resolved fluorescence studies are consistent with reversible excited-state intramolecular proton transfer in 4′-dialkylamino-3-hydroxyflavone, J. Phys. Chem. A 107 (2003) 9522–9529.
[26] A.S. Klymchenko, G. Duportail, Y. Mely, A.P. Demchenko, Ultrasensitive two-color fluorescence probes for dipole potential in phospholipid membranes, Proc. Natl. Acad. Sci. U. S. A. 100 (2003) 11219–11224.
[27] A.S. Klymchenko, V.G. Pivovarenko, T. Ozturk, A.P. Demchenko, Modulation of the solvent-dependent dual emission in 3-hydroxychromones by substituents, New J. Chem. 27 (2003) 1336–1343.
[28] A.S. Klymchenko, G. Duportail, A.P. Demchenko, Y. Mely, Bimodal distribution and fluorescence response of environment-sensitive probes in lipid bilayers, Biophys. J. 86 (2004) 2929–2941.
[29] A.S. Klymchenko, Y. Mely, A.P. Demchenko, G. Duportail, Simultaneous probing of hydration and polarity of lipid bilayers with 3-hydroxyflavone fluorescent dyes, Biochim. Biophys. Acta 1665 (2004) 6–19.
[30] A.S. Klymchenko, G. Duportail, T. Ozturk, V.G. Pivovarenko, Y. Mely, A.P. Demchenko, Novel two-band ratiometric fluorescence probes with different location and orientation in phospholipid membranes, Chem. Biol. 9 (2002) 1199–1208.